*Proc. Natl. Acad. Sci. USA*
Vol. 90, pp. 11588–11592, December 1993
Biochemistry

# Functional expression of P-glycoprotein encoded by the mouse *mdr3* gene in yeast cells

STEPHAN RUETZ*, MARTINE RAYMOND†, AND PHILIPPE GROS*‡

*Department of Biochemistry, McGill University, Montreal, PQ, Canada, H3G 1Y6; and †Biotechnology Research Institute, Montreal, PQ, Canada, H4P 2R2

*Communicated by Randy Schekman, August 31, 1993 (received for review May 27, 1993)*

**ABSTRACT** **We have expressed P-glycoprotein (P-gp) encoded by the mouse *mdr3* gene in the yeast *Saccharomyces cerevisiae* and have developed an experimental protocol to isolate and purify inside-out plasma membrane vesicles (IOVs) from these cells. Biochemical characterization of IOVs from control and P-gp-expressing cells isolated by this procedure show that they are greatly enriched for plasma membrane markers, are tightly sealed, and are competent for D-glucose transport. P-gp expression in these vesicles results in the appearance of a specific ATP-dependent and temperature-sensitive transport of the drugs colchicine and vinblastine that is osmotically sensitive. P-gp-mediated drug transport into these IOVs is inhibited by a known P-gp modulator, verapamil, and can be abrogated by prior incubation of the IOVs with an anti-P-gp antibody. A Ser-939 → Phe mutation within the predicted transmembrane domain 11 of P-gp, which is known to modulate its function in mammalian cells, drastically reduces drug transport in IOVs obtained from yeast cells expressing the mutant protein. The successful demonstration of active drug transport into IOVs from P-gp-expressing yeast cells indicates that P-gp can mediate both chemotherapeutic drugs and a-pheromone transport in yeast cells.**

Multidrug resistance (MDR) is caused *in vitro* and *in vivo* by overexpression of a membrane phosphoglycoprotein, P-glycoprotein (P-gp) (1). P-gp is encoded by a small family of related *mdr* genes composed of three members in rodents (*mdr1*, *mdr2*, and *mdr3*) (2–4) and two in humans (*MDR1* and *MDR2*; now designated *PGY1* and *PGY2*) (5, 6). The prototype P-gp is formed by two homologous halves, each composed of six predicted transmembrane domains and one nucleotide-binding (NB) fold (7). The P-gp family is also part of a very large family of ATP-binding cassette membrane transporters (8) with members in prokaryotes and lower and higher eukaryotes, including the yeast *Saccharomyces cerevisiae* a peptide pheromone transporter STE6 (9).

The exact mechanism of P-gp action remains largely unsolved. A considerable body of evidence suggests that P-gp acts as a membrane-bound, ATP-dependent drug efflux pump that reduces intracellular drug accumulation in resistant cells. These include the observations that (*i*) P-gp expression in *mdr* transfectants causes both reduced accumulation and increased cellular efflux of MDR drugs, both of which are ATP dependent (1); (*ii*) P-gp binds photoactivatable ATP analogs (10) and shows ATPase activity (11), and mutations in either of its two predicted NB sites abrogate function (12); (*iii*) P-gp binds photoactivatable drug analogs (13), and mutations in its predicted transmembrane domains modulate substrate specificity and alter drug binding (14, 15); and (*iv*) P-gp shows structural and functional homology with a number of ATP-binding cassette transport proteins implicated in the transmembrane transport of structurally heterogeneous substrates, such as peptides, ions, sugars, and fatty acids (16). Recently, additional and/or alternative biological activities have been attributed to P-gp in drug-resistant cells, such as the osmotic-sensitive $Cl^-$ channel (17), ATP carrier (18), intracellular pH regulator (19), and lipid flippase (20). Purification and reconstitution of P-gp in proteolipososomes will be required to analyze these various transport activities and determine how they may contribute to P-gp-mediated drug resistance. Finally, the specific protein domains and amino acid residues involved in (*i*) recognition of structurally dissimilar substrates, (*ii*) signal transduction from the NB sites, (*iii*) and membrane helix packing all remain poorly identified. In the absence of three-dimensional protein structure information, an expression system allowing rapid and extensive genetic analysis of P-gp is needed to carry out structure–function analysis of this protein.

Although the human MDR1 polypeptide has been successfully overexpressed in yeast cells, the consequences of this expression on drug resistance and/or drug transport in these cells remain unclear, causing either increased (21) or decreased (22) cellular drug resistance. Recently, we have demonstrated that P-gp encoded by the mouse *mdr3* gene is not only structurally related to the yeast pheromone transporter STE6 but is also functionally similar since *mdr3* can restore mating in a yeast mutant carrying a null allele at the *STE6* locus (9). To pursue the characterization of P-gp expressed in *S. cerevisiae*, an experimental protocol for isolating tightly sealed plasma membrane (PM) vesicles of inverted polarity has been elaborated. The effect of expressing wild-type or mutant P-gps on the kinetics of MDR drug accumulation in these vesicles has been analyzed.

## MATERIALS AND METHODS

**Material.** Zymolyase 100T was purchased from ICN; Con A and Con A-Sepharose were obtained from Pharmacia; [G-$^3$H]vinblastine (VBL) sulfate (11.7 Ci/mmol; 1 Ci = 37 GBq), [*ring A*, 4-$^3$H]colchicine (COL; 8.2 Ci/mmol), and D-[6-$^3$H]glucose (25 Ci/mmol) were from Amersham; and ribo- and deoxyribonucleases and protease inhibitors were obtained from Boehringer Mannheim.

**Cells and Growth Conditions.** *S. cerevisiae* cells of strain JPY201 transformed with plasmids pVT, pVT-mdr3S (mdr3S), and pVT-mdr3F (mdr3F) were grown to midlogarithmic phase ($OD_{600}$ of 1.5–2.0) at 30°C in selective synthetic medium lacking uracil. Growth was stopped by addition of 10 mM $NaN_3$, and cultures were then chilled in ice water. Cells were collected by centrifugation (8275 × *g*, 10 min), washed once in 10 mM Tris·HCl, pH 7.5/1 mM dithiothreitol/5 mM $NaN_3$/5 mM EDTA, and stored at −70°C in 2- to 3-g aliquots.

**Isolation of Plasma Membrane Vesicles.** For the isolation of membrane vesicles, all steps were performed at 0°C–4°C using ice-cold buffers and solutions supplemented with pro-

The publication costs of this article were defrayed in part by page charge payment. This article must therefore be hereby marked "*advertisement*" in accordance with 18 U.S.C. §1734 solely to indicate this fact.

Abbreviations: P-gp, P-glycoprotein; IOV, inside-out plasma membrane vesicle; VBL, vinblastine; COL, colchicine; PM, plasma membrane; MDR, multidrug resistance; NB, nucleotide binding.

‡To whom reprint requests should be addressed.

tease inhibitors: phenylmethylsulfonyl fluoride (1 mM), pepstatin (1 μg/ml), leupeptin (1 μg/ml), aprotinin (1 μg/ml). Yeast spheroplasts were prepared by Zymolyase digestion (1 mg/g of wet cells, 45 min at 30°C) in SM buffer (1.2 M sorbitol/20 mM Hepes-KOH, pH 7.0/2 mM EDTA) as described (9). Spheroplasts were washed twice (2000 × g, 10 min) in SM buffer, resuspended in 8 ml of a buffer (10 mM $MgCl_2$/2 mM $CaCl_2$/2 mM $MnSO_4$/0.25 M mannitol/50 mM Tris·HCl, pH 7.5) containing 2 mg of Con A, and incubated for 10 min on ice. Con A-coated spheroplasts were concentrated by centrifugation (300 × g, 10 min) through a cushion of 10 mM $MgCl_2$/0.5 M mannitol/50 mM Tris·HCl, pH 7.5 and resuspended in hypotonic lysis buffer (5 mM $MgSO_4$/10 mM Tris·HCl, pH 7.5) supplemented with 1 mM phenylmethylsulfonyl fluoride and ribo- and deoxyribonuclease at 50 and 10 μg/ml, respectively. After a 30-min incubation, the spheroplasts were collected by centrifugation (8275 × g, 10 min), resuspended in lysis buffer containing protease inhibitors, and further disrupted by Dounce homogenization (15–20 strokes). Membrane and cell fragments were collected (1000 × g, 10 min) by centrifuging the suspension again through a mannitol cushion (as above), and the resulting pellet was suspended in 2.5 ml of 50% (vol/vol) glycerol/5 mM $MgSO_4$/10 mM Tris·HCl, pH 7.5, and stored at −70°C.

To convert the isolated membrane sheets into vesicles, the frozen membrane fraction was thawed on ice, washed twice with lysis buffer, and resuspended in the same buffer (final volume of 7.5 ml) containing 0.6 M α-methylmannoside. The suspension was pressed through a 23-gauge needle and layered over 8 ml of a buffer consisting of 20% sucrose, 0.2 mM $CaCl_2$, and 10 mM Tris·HCl (pH 7.5) and centrifuged (750 × g, 30 min). Material that banded at the interface was removed, diluted with vesicle buffer (VB1 buffer; 200 mM sucrose/25 mM potassium gluconate/0.2 mM $CaCl_2$/10 mM Tris·HCl, pH 7.5) and collected by centrifugation (17,200 × g, 15 min). The resulting pellet was resuspended with the aid of a syringe (26.5-gauge needle) in 3 ml of VB1 buffer supplemented with 2 mM $CaCl_2$ and 5 mM $MnSO_4$ and applied to 2 ml of Con A-Sepharose beads preequilibrated in a 5-ml column with 10 bed volumes of the same buffer. After a 30-min incubation at 4°C, unbound inside-out PM vesicles (IOVs) were collected by gravity flow and further concentrated by centrifugation (17,200 × g, 15 min). The final IOV fraction was resuspended in VB1 buffer (100–500 μl).

**Vesicle Transport Assays.** [$^3$H]VBL and [$^3$H]COL uptake measurements into IOVs were determined by a rapid filtration technique. IOVs were diluted to 8–12 mg of protein per ml with VB1 buffer supplemented with creatine phosphokinase (3 μg/ml), and drug transport was initiated by diluting a 10-μl aliquot of this suspension in 90 μl of a prewarmed (37°C) transport buffer (TB1 buffer; 10 mM $MgCl_2$/25 mM potassium gluconate/2.5 mM NaATP/10 mM creatine phosphate/200 mM sucrose/10 mM Tris·HCl, pH 7.5) containing either [$^3$H]VBL (11.7 mCi/mmol) or [$^3$H]COL (8.2 mCi/mmol) at a final concentration of 1 μM. Transport was terminated by the addition of 2 ml of ice-cold VB1 buffer, and vesicle-associated radioactivity was determined by immediate filtration through a 0.65-μm nitrocellulose filter (type HA; Millipore) preequilibrated in VB1 buffer containing 5 μM VBL. After two additional washes with 2 ml of VB1 solution, the vesicle-associated radioactivity was determined by liquid scintillation counting. All data are the mean values ± SD of triplicates of two (Figs. 3 and 4) or three (Fig. 2) independent IOV preparations.

For D-[$^3$H]glucose transport assays, IOVs were equilibrated for 90 min at 25°C in VB2 buffer (100 mM sucrose/25 mM potassium gluconate/0.2 mM $CaCl_2$/10 mM Tris·HCl, pH 7.5) containing either 100 mM D- or L-glucose. D-[$^3$H]Glucose transport into IOVs was performed as described for drug transport, except that IOVs were diluted 20-fold with TB2 buffer (25 mM potassium gluconate/200 mM sucrose/10 mM Tris·HCl, pH 7.5) containing a final concentration of D-glucose of 5 mM and D-[$^3$H]glucose (25 μCi/mmol).

**Analytical Methods.** The ATPase activity in IOV and ghost fractions was measured as described elsewhere (23). Membrane suspensions (0.3 mg/ml) in VB1 buffer were diluted with an equal volume of VB1 buffer containing 5 mM NaATP and 10 mM $MgCl_2$ (omitted in the presence of EDTA) and incubated at 37°C for 20 min. The reactions were stopped by addition of ice-cold 1% SDS/2% $H_2SO_4$/0.5% ammonium molybdate, and 100-μl aliquots (3–4 μg of protein) were added to 50 μl of 1% ascorbic acid and further incubated 30 min at 25°C. Optical density was determined at 660 nm using an ELISA reader (Bio-Rad). Protein concentrations were determined according to Bradford in the presence of 5% formic acid.

## RESULTS AND DISCUSSION

**Isolation and Characterization of IOVs.** The primary goal of this study was to functionally express P-gp in yeast cells. For this, it was necessary to devise an experimental protocol to isolate IOVs where P-gp-mediated drug transport could be assayed. The procedure used is based on a method that was originally described to purify inverted PM vesicles from the eukaryote *Neurospora crassa* (24, 25) and that was previously adapted to isolate yeast PM fractions (26, 27). The protocol involves coating the surface of yeast spheroplasts with Con A to stabilize the plasma membrane, preventing fragmentation and spontaneous revesiculation upon osmotic lysis of the cells. This treatment also allows physical separation of large lectin-coated membrane sheets (ghosts) from other cellular constituents by low-speed centrifugation. After removal of Con A with excess of α-methylmannoside, these open membrane sheets are then converted to closed vesicles, which can be recovered by isometric centrifugation. The resulting vesicles are finally subfractionated by affinity chromatography into inside-out and right-side-out vesicles.

Yeast strain JPY201 transformed either with control plasmid pVT or with the same plasmid carrying full-length cDNAs for the mouse *mdr3* gene (mdr3S) or a mutant *mdr3* gene (mdr3F) with reduced activity was used in all experiments. Starting with 2–3 g of yeast cells, we could routinely obtain 20–30 mg of the ghost fraction and 0.4–0.6 mg of the final vesicular fraction (8% and 0.4% of the starting material). Examination of the final membrane fraction by electron microscopy showed that it contained unilamellar vesicles with a mean diameter ranging from 1.5 to 3 μm (data not shown). To initiate characterization of this membrane fraction and analyze the polarity of the vesicles, we used the vanadate-sensitive $H^+$-ATPase as a specific plasma membrane enzymatic marker (28) (Table 1). Vesicle preparations from the three yeast transformants (pVT, mdr3S, and mdr3F) showed similar amounts of a net $Mg^{2+}$-dependent release of inorganic phosphate ($P_i$) (the calculated value of 128.2–138.8 nmol·mg$^{-1}$·min$^{-1}$ was set at 100%). Addition of vanadate completely abolished ATP hydrolysis (4–6%), with the amounts of $P_i$ released (63 nmol·mg$^{-1}$·min$^{-1}$) similar to background levels (60 nmol·mg$^{-1}$·min$^{-1}$) measured in the negative controls in the absence of $Mg^{2+}$ (+EDTA) or where ATP had been replaced by AMP (data not shown). The specific activity of this ATPase measured in our vesicle preparations is lower than the 250–700 milliunits/mg (1 unit = 1 μmol of $P_i$ released per min) value reported for whole PM preparations. This difference results from the higher pH (7.5) used in our ATPase measurements and subsequent drug transport assays (optimal pH for P-gp ATPase activity), at which the activity of the PM $H^+$-ATPase is reduced by 60% over its maximal activity measured at pH 6 (29). $Mg^{2+}$-dependent ATP hydrolysis was also measured in these vesicles in the presence of

Table 1. $Mg^{2+}$-dependent ATPase activities in isolated yeast membrane fractions

| Inhibitor | Specific ATPase activity, nmol of $P_i$ per mg per min | | | Relative ATPase activity,† % | | |
|---|---|---|---|---|---|---|
| | pVT | mdr3F | mdr3S | pVT | mdr3F | mdr3S |
| None (control) | 196.97 | 198.55 | 187.63 | 100 | 100 | 100 |
| EDTA,* 10 mM | 64.31 | 57.48 | 58.69 | 0 | 0 | 0 |
| Vanadate, 20 μM | 69.08 | 63.69 | 65.23 | 4 | 5 | 6 |
| Triton X-100, 0.05% | 194.04 | 187.73 | 182.29 | 102 | 93 | 97 |
| DES, 100 μM | 97.39 | 96.58 | 95.96 | 24 | 29 | 29 |
| MN, 200 μM | 86.28 | 96.61 | 95.95 | 16 | 10 | 14 |
| Azide, 10 mM | 191.57 | 203.66 | 185.78 | 95 | 107 | 98 |
| EDAC, 100 μM | 186.03 | 181.12 | 191.57 | 93 | 93 | 95 |

Maximal $Mg^{2+}$-dependent, EDTA-sensitive ATPase activity (release of $P_i$ during a 20-min reaction) was calculated for each group and set at 100%. The modulatory effect of various inhibitors was measured and is expressed as a percentage of the maximal ATPase activity. Data are values of three determination of three independent preparations. Relative error on average measurements was between 1% and 6%. DES, diethylstilbestrol; EDAC, 1-ethyl-3-(3-dimethylaminopropyl)carbodiimide; MN, miconazole nitrate.
*$Mg^{2+}$ was omitted.
†Relative to the control.

Triton X-100 added to a final concentration of 0.05%. At this concentration, Triton X-100 only permeabilizes rather than solubilizes membrane vesicles, therefore permitting access to masked ATPases present in right-side-out oriented vesicles. This treatment had no effect on the overall ATPase activity (Table 1), suggesting that the majority of the isolated vesicles were in the inverted orientation (IOVs).

Since vanadate is also a potent inhibitor of other ATPases as well as acid and alkaline phosphatases (29), the effect of additional inhibitors of PM $H^+$-ATPase was investigated. Both diethylstilbestrol (29) and miconazole nitrate (29) strongly inhibit ATP hydrolysis in these vesicles, causing a 75% and 85% reduction in $P_i$ release (Table 1), respectively. In contrast, sodium azide, a specific inhibitor of the mitochondrial $H^+$-ATPase, and 1-ethyl-3-(3-dimethylaminopropyl)carbodiimide, an inhibitor of the vacuolar $H^+$-ATPase (29), do not affect the overall $Mg^{2+}$-dependent ATP hydrolysis. These results indicate that the vesicle preparations contain PMs primarily and are significantly depleted of mitochondrial and vacuolar membranes. Finally, the effect of the inhibitors on ATPase activity was also tested in the ghost membrane fraction to deduce a relative enrichment factor for the three major ATPases. The final purification steps used to isolate the PM vesicle fraction resulted in a 6- to 7-fold enrichment in PMs with a combined residual mitochondrial and vacuolar contamination of <10% (data not shown). A comparison of data obtained for pVT, mdr3F, and mdr3S indicates that the ATPase activity of P-gp could not be detected in our IOV preparations (Table 1), even after treatment with VBL or verapamil (data not shown), both known modulators of P-gp ATPase activity (30). P-gp ATPase activity is possibly masked by the strong activity of the PM $H^+$-ATPase.

The structural integrity of the isolated PM vesicles and their capacity to carry out transport were then tested. For this, we measured D-glucose influx/counterflow in vesicles from JPY201 cells transformed with either pVT, mdr3S, or mdr3F (Fig. 1) (27). Vesicles were preloaded with 100 mM D-glucose, and D-[$^3$H]glucose countertransport was initiated by diluting the suspension 20-fold with a buffer containing tracer D-[$^3$H]glucose (Fig. 1). Under these conditions, D-[$^3$H]glucose uptake in the vesicles is rapid and exhibits a characteristic "overshoot" profile of accumulation. The counterflow phenomenon is temperature dependent and

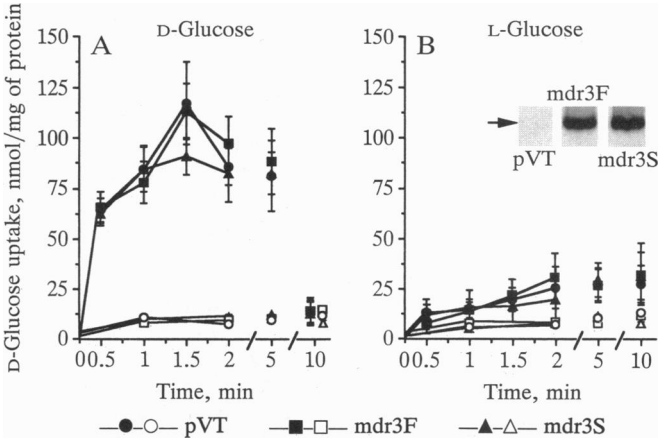


FIG. 1. D-Glucose countertransport in plasma membrane vesicles from control and *mdr3*-expressing yeast cells. IOVs were preloaded (90 min, 25°C) in VB2 buffer containing either 100 mM D-glucose (*A*) or L-glucose (*B*). D-[$^3$H]Glucose countertransport (0°C, open symbols; 37°C, filled symbols) was measured by diluting the IOV suspension in TB2 buffer containing D-[$^3$H]glucose (25 mCi/mmol). Data are the mean ± SD of triplicates (37°C) and duplicates (0°C) of two independent IOV preparations. (*Inset*) Aliquots (25 μg) of IOVs from control (*p*VT) and *mdr3*-expressing (mdr3S and mdr3F) cells were immunoblotted and incubated with the monoclonal anti-Pgp antibody C219.

completely abolished at 0°C. The counterflow is specific and is not observed when the vesicles are preloaded with L-glucose (Fig. 1) and is abolished by increasing osmolarity to 1 M sucrose (data not shown). Finally, the kinetics of D-[$^3$H]glucose accumulation into vesicles of control cells and mdr3S and mdr3F transformants, which as shown by immunoblotting (Fig. 1 *Inset*) contain equivalent amounts of expressed wild-type or mutant P-gp, are identical. [The levels of P-gps expression in the yeast IOVs were similar to that of drug-resistant CHO cells overexpressing the corresponding P-gps (15).] This indicates that P-gp expression does not alter uptake or retention of glucose in these vesicles. Thus, the enzymatic data combined with the results of the D-[$^3$H]glucose counterflow experiments clearly confirm that the isolated PM vesicles are inverted (IOVs), tightly sealed, and functionally competent for transport.

**[$^3$H]VBL and [$^3$H]COL Uptake into IOV Fractions.** The kinetics of MDR drug accumulation into control (pVT) or *mdr3*-expressing (mdr3S or mdr3F) IOVs were tested using [$^3$H]VBL and [$^3$H]COL as substrates. Although the three vesicle preparations show similar kinetics of glucose counterflow, they exhibit strikingly different profiles of VBL and COL accumulation (Fig. 2). While little if any VBL accumulation is detected in control pVT IOVs, mdr3S IOVs accumulate VBL rapidly over the 10-min time course, with a maximal accumulation of 5- to 6-fold above background (pVT control). The kinetics of COL transport in these vesicles are similar to those measured for VBL, with no accumulation in pVT IOVs and rapid accumulation in mdr3S IOVs, reaching a maximum 10–15 min after initiation of transport (10-fold increase above background). The Ser-939 → Phe substitution in P-gp TM 11 (mdr3F IOVs) causes 75% reduction in VBL accumulation and a complete abrogation of COL uptake in IOVs from mutant-expressing cells (Fig. 2). The modulatory effect of this mutation on *mdr3*-mediated drug accumulation in yeast IOVs is in excellent agreement with our previous biochemical characterization of this mutation in mammalian cells, where it causes partial loss of VBL resistance and complete abrogation of COL resistance (15, 31). Drug accumulation into mdr3S and mdr3F IOVs is completely inhibited by vanadate, a known inhibitor of several ATPases, including

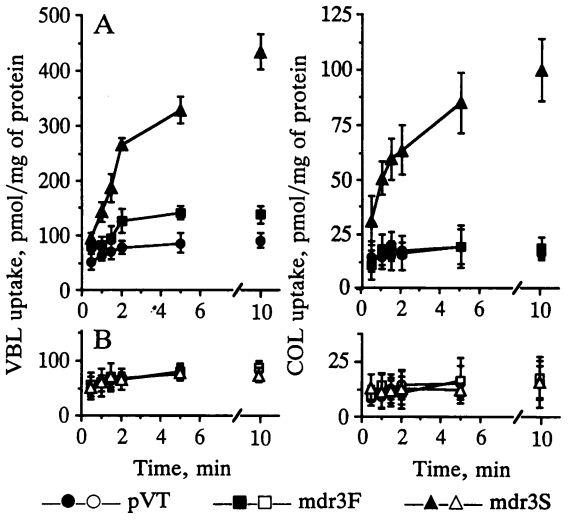


FIG. 2. Kinetics of drug transport into IOVs from control and *mdr3*-expressing yeast cells. Drug transport was measured by diluting the IOVs in TB1 buffer containing either [$^3$H]VBL (11.7 mCi/mmol; *Left*) or [$^3$H]COL (8.2 mCi/mmol; *Right*) in the absence (*A*) or presence (*B*) of vanadate (100 μM).

P-gp (30). The amount of vanadate-insensitive drug binding to IOVs was identical in the three IOV populations but was 4 times higher for VBL than for COL (50 vs. 12.5 pmol/mg). This value most likely represents nonspecific drug binding to IOVs, and the difference between VBL and COL probably reflects the higher lipophilicity of VBL (32). Together, the data indicate that expression of P-gp in the plasma membrane of *S. cerevisiae* causes the appearance of a vanadate-sensitive drug transport mechanism. Moreover, the modulatory effect of a point mutation on *mdr3* function analyzed in mammalian cells is qualitatively and quantitatively reflected in purified yeast IOVs.

**Temperature and Osmotic Sensitivity of VBL Uptake.** To determine if enhanced drug accumulation in mdr3S IOVs is energy-dependent transport, as opposed to nonspecific effects of P-gp expression on drug diffusion into IOVs, we analyzed the temperature dependence and osmotic sensitivity of drug transport. First, VBL uptake into mdr3S IOVs was carried out at 37°C, 25°C, and 0°C. As shown in Fig. 3*A*, lowering the temperature from 37°C to 25°C results in a 50% reduction in the rate of VBL accumulation in the IOVs. Reducing the assay temperature to 0°C completely abolished

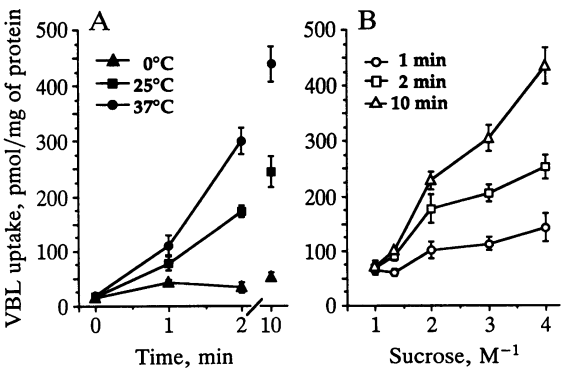


FIG. 3. Temperature (*A*) and osmotic (*B*) sensitivity of VBL transport into IOVs from *mdr3S*-expressing cells. (*A*) VBL transport was performed as in Fig. 2 at either 0°C, 25°C, or 37°C. (*B*) IOVs were initially resuspended in VB1 buffer containing increasing concentrations of sucrose (0.25–1 M). VBL uptake was measured at 1-, 2-, and 10-min intervals in TB1 buffer (37°C) adjusted with identical concentrations of sucrose.

drug accumulation into mdr3S IOVs. The results indicate that VBL transport is mediated by a temperature-dependent, carrier-mediated transport process. Second, we determined whether VBL accumulation in mdr3S IOVs is proportional to the intravesicular volume, which can be reduced by increasing the sucrose concentration outside the vesicles. Therefore, VBL transport was measured into mdr3S IOVs resuspended in VB buffer containing increasing concentrations of sucrose (Fig. 3*B*). The results indicate that VBL uptake is inversely proportional to the sucrose concentration in the transport buffer and therefore to the intravesicular volume. At 1 M sucrose, no drug accumulation is detected over the 10-min incubation assay, with a final VBL uptake of 50–60 pmol/mg of protein. This value is similar to that measured in normal conditions in control pVT IOVs (Fig. 2) or in mdr3S IOVs treated with vanadate (Fig. 2) and most likely represents initial nonspecific drug binding to the vesicles. Together, these data are compatible with osmotic sensitive drug accumulation in the intravesicular space of mdr3S IOVs. However, the high degree of hydrophobicity and high lipid partition coefficient of VBL (32) limit the interpretation of sensitivity of transport to osmolarity.

**Effect of Inhibitors on P-gp-Mediated Drug Transport in Yeast IOVs.** To further characterize the drug transport activity detected in mdr3S and mdr3F IOVs, the effect of several inhibitors on VBL transport was monitored (Fig. 4). The effect of the protonophore carbonylcyanide *m*-chlorophenylhydrazone was first measured. IOVs contain significant amounts of the vanadate-sensitive PM H$^+$-ATPase, which generates a proton electrochemical gradient ($\Delta\mu_{H^+}$, interior positive and/or acid) that could drive accumulation of MDR drugs (32). The results shown in Fig. 4 clearly show that this is not the case, as carbonylcyanide *m*-chlorophenylhydrazone has no effect on VBL accumulation in mdr3S or mdr3F IOVs. In mammalian cells, P-gp-mediated drug resistance is strictly dependent on intact intracellular pools of nucleotide triphosphates (1). Indeed, P-gp has two predicted NB sites, both of which are absolutely required for function (12). Finally, the ATPase activity of P-gp also seems to be required for biological activity (12, 30). Therefore, the requirement for ATP of the *mdr3*-induced VBL transport in

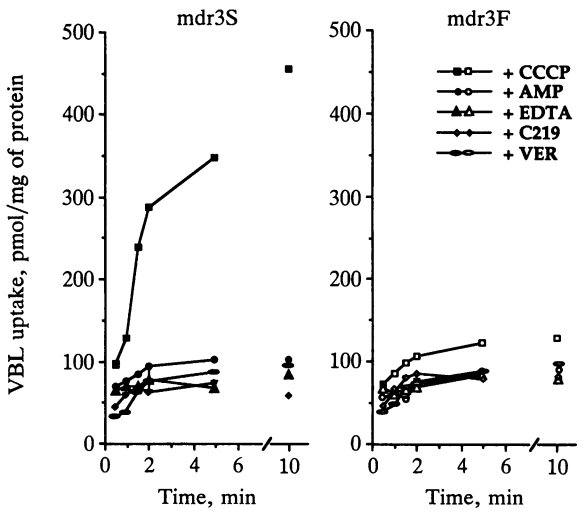


FIG. 4. Characterization of VBL transport into IOVs from *mdr3*-expressing yeast cells. Modulation of VBL transport either by addition of carbonylcyanide *m*-chlorophenylhydrazone (10 μM) or verapamil (VER; 20 μM), substitution of NaATP by NaAMP (2.5 mM), or replacement of $MgCl_2$ by EDTA (10 mM) was measured. Finally, the effect on VBL accumulation of prior incubation of the IOVs with the mouse anti-P-gp monoclonal antibody C219 (1:300 dilution, 30 min at 25°C) was determined. Relative errors were <5% (not shown for clarity).

IOVs was investigated (Fig. 4). Enhanced VBL accumulation in mdr3S IOVs is strictly ATP dependent and requires ATP hydrolysis since neither AMP (Fig. 4) nor the nonhydrolyzable ATP analogue adenosine 5′-[thio]triphosphate (data not shown) supports VBL transport. In addition, omission of the divalent cation $Mg^{2+}$ from the transport buffer completely abolishes VBL transport into mdr3S IOVs. P-gp action can be inhibited by a series of structurally heterogeneous compounds such as verapamil, trifluoperazine, progesterone, cyclosporin A, and many others (33). The possible modulatory effect of one such agent, verapamil, was tested here (Fig. 4). As shown, verapamil completely inhibits VBL accumulation into mdr3S IOVs. Finally, the effect of a specific anti-P-gp antibody on VBL transport into mdr3S IOVs was evaluated. Mouse anti-P-gp monoclonal antibody C219 recognizes the epitope VVQEALD, which is located immediately downstream of each of the two predicted NB sites of P-gp (34). Structural predictions and epitope-mapping studies suggest that these sites are located on the intracellular face of the membrane of intact cells (16). Therefore, in IOVs, these sites should be exposed to the outside and should be readily accessible to an antibody such as C219. Results in Fig. 4 show that preincubation of the mdr3S IOVs for 30 min at 25°C with C219 abolishes drug transport.

## CONCLUSION

We have developed an experimental protocol for the isolation of yeast plasma membrane vesicles of inverted orientation containing functional P-gp. The system catalyzes ATP-dependent, verapamil-sensitive drug transport with all the characteristics of P-gp-mediated drug transport in mammalian cells, including inhibition of transport by anti-Pgp antibodies. In addition, the modulatory effect of a single point mutation on *mdr3* function (overall activity and substrate specificity) reported for intact mammalian cells (31) has been qualitatively and quantitatively reproduced in IOVs expressing the corresponding wild-type and mutant proteins. The results reflect proper membrane insertion and targeting of mammalian P-gp in yeast cells, leading to preservation of functional characteristics of P-gp-mediated drug transport in yeast IOVs. This functional expression system provides an ideal experimental tool for in-depth biochemical and pharmacological characterization of P-gp function. Specifically, the mechanism of P-gp action remains unknown and can only be solved by purification of P-gp to homogeneity, followed by reconstitution into lipid vesicles. Although recent attempts in this direction show promising results, they are hampered by the limited availability of starting material from either drug-resistant cell lines (35) or insect cells overexpressing large amounts of recombinant protein (30, 36). The yeast expression system described here should allow the rapid and simplified production of large amounts of biologically active P-gp, alleviating a key problem to purification and reconstitution.

Recently, we have shown that the structural homology detected between mammalian P-gp and its yeast homolog STE6 translates into functional homology since *mdr3S* can complement a null allele at the *STE6* locus (9). In addition, we observed that transport of the **a** peptide pheromone by mdr3S in these cells is mechanistically similar to drug transport by mdr3S in mammalian cells, since the mdr3F mutant is inactive in the *STE6* complementation assay. These data together with those reported here demonstrate that P-gp can transport both MDR drugs and the peptide pheromone **a** in yeast. The availability of a quick assay to monitor *mdr3* complementation in haploid yeast cells (9) allows for rapid functional screening of P-gp mutants obtained by random or targeted mutagenesis and should also permit the production and characterization of intragenic suppressor mutations. The parallel effect of such mutations on P-gp-mediated drug transport can be readily established in IOVs. Therefore, the yeast model should greatly facilitate the structure–function analysis of P-gp by classical genetic means, a key experimental approach in the absence of three-dimensional structure. Finally, the model system described here should allow functional analysis of other members of the ABC superfamily of transport proteins, including CFTR (37), TAP1/TAP2 (38), and PMP70/ALDP (39).

This work was supported by research grants to P.G. from the National Cancer Institute of Canada. S.R. is supported by the Schweiz. Krebsliga, and M.R. is supported by a scholarship from the Medical Research Council of Canada. P.G. is an International Scholar from the Howard Hughes Medical Institute.

1. Endicott, J. A. & Ling, V. (1989) *Annu. Rev. Biochem.* **58,** 137–171.
2. Gros, P., Neriah, Y. B., Croop, J. M. & Housman, D. E. (1986) *Nature (London)* **323,** 728–731.
3. Gros, P., Raymond, M., Bell, J. & Housman, D. E. (1988) *Mol. Cell. Biol.* **8,** 2770–2778.
4. Devault, A. & Gros, P. (1990) *Mol. Cell. Biol.* **10,** 1652–1663.
5. Chen, C. J., Chin, J. E., Ueda, K., Clark, D. P., Pastan, I., Gottesman, M. M. & Roninson, I. B. (1986) *Cell* **47,** 381–389.
6. Van der Bliek, A. M., Kooiman, P. H., Schneider, C. & Borst, P. (1988) *Gene* **71,** 407–411.
7. Gros, P., Croop, J. & Housman, D. E. (1986) *Cell* **47,** 371–380.
8. Higgins, C. F., Hyde, S. C., Mimmack, M. M., Gileadi, U. & Gill, D. R. (1990) *J. Bioenerg. Biomembr.* **22,** 571–592.
9. Raymond, M., Gros, P., Whiteway, M. & Thomas, D. Y. (1992) *Science* **256,** 232–234.
10. Schurr, E., Raymond, M., Bell, J. & Gros, P. (1989) *Cancer Res.* **49,** 2729–2734.
11. Hamada, H. & Tsuruo, T. (1988) *J. Biol. Chem.* **263,** 1454–1458.
12. Azzaria, M., Schurr, E. & Gros, P. (1989) *Mol. Cell. Biol.* **9,** 5289–5297.
13. Safa, A. R. (1992) *Cancer Res.* **10,** 295–305.
14. Safa, A. R., Stern, R. K., Choi, K., Agresti, M., Iamai, I., Metha, N. D. & Roninson, I. B. (1990) *Proc. Natl. Acad. Sci. USA* **87,** 7225–7229.
15. Kajiji, S., Talbot, F., Grizzuti, K., Van Dyke-Phillips, V., Agresi, M., Safa, A. R. & Gros, P. (1993) *Biochemistry* **32,** 4185–4194.
16. Gros, P. & Buschman, E. (1993) *Int. Rev. Cytol. C* **137,** 169–197.
17. Valverde, M. A., Diaz, M., Sepulveda, F. V., Gill, D. R., Hyde, S. C. & Higgins, C. F. (1992) *Nature (London)* **355,** 830–833.
18. Abraham, E. H., Prat, A. G., Gerweck, L., Seneveratne, T., Arceci, R. J., Kramer, R., Guidotti, G. & Cantiello, H. F. (1993) *Proc. Natl. Acad. Sci. USA* **90,** 312–316.
19. Roepe, P. D. (1992) *Biochemistry* **31,** 12555–12564.
20. Higgins, C. F. & Gottesmann, M. M. (1992) *Trends. Biochem. Sci.* **17,** 18–19.
21. Kuchler, K. & Thorner, J. (1992) *Proc. Natl. Acad. Sci. USA* **89,** 2302–2306.
22. Saeki, T., Shimabuku, A. M., Azuma, Y., Shibano, Y., Komano, T. & Ueda, K. (1991) *Agric. Biol. Chem.* **85,** 1859–1865.
23. Sarkadi, B., Szasz, I., Gerloci, A. & Gardos, V. (1977) *Biochim. Biophys. Acta* **464,** 93–107.
24. Scarborough, G. A. (1975) *J. Biol. Chem.* **250,** 1106–1111.
25. Scarborough, G. A. (1980) *Biochemistry* **19,** 2925–2931.
26. Tschopp, J. & Schekman, R. (1983) *J. Bacteriol.* **156,** 222–229.
27. Franzusoff, A. J. & Cirillo, V. P. (1983) *J. Biol. Chem.* **258,** 3608–3614.
28. Willsky, G. R. (1979) *J. Biol. Chem.* **254,** 3326–3332.
29. Serrano, R. (1991) *The Molecular and Cellular Biology of the Yeast Saccharomyces: Genome Dynamics, Protein Synthesis, and Energetics* (Cold Spring Harbor Lab. Press, Plainview, NY), pp. 523–585.
30. Sarkadi, B., Price, E. M., Boucher, R. C., Germann, U. A. & Scarborough, G. A. (1992) *J. Biol. Chem.* **267,** 4854–4858.
31. Gros, P., Dhir, R., Croop, J. & Talbot, F. (1991) *Proc. Natl. Acad. Sci. USA* **88,** 7289–7293.
32. Zamora, J. M., Pearce, H. L. & Beck, W. T. (1988) *Mol. Pharmacol.* **33,** 454–462.
33. Beck, W. T. (1990) *Eur. J. Cancer* **26,** 513–515.
34. Georges, E., Bradly, G., Gariepy, J. & Ling, V. (1990) *Proc. Natl. Acad. Sci. USA* **87,** 152–157.
35. Doige, C. A., Xiaohong, Y. & Sharom, F. J. (1993) *Biochim. Biophys. Acta* **1109,** 149–160.
36. Germann, U. A., Willingham, M. C., Pastan, I. & Gottesmann, M. M. (1990) *Biochemistry* **29,** 2295–2303.
37. Riordan, J. R., Rommens, J. M., Kerem, B. S., Alon, N., Rozmahel, R., Grezelczak, Z., Zielenski, J., Lok, S., Plasviic, N., Chou, J. L., Drumm, M. L., Iannuzzi, M. C., Collins, F. S. & Tsui, L. C. (1989) *Science* **245,** 1066–1073.
38. Spies, T. & De Mars, R. (1991) *Nature (London)* **351,** 323–324.
39. Vall, D. & Gaernter, J. (1993) *Nature (London)* **361,** 682–683.